Inorganic Chemistry

pubs.acs.org/IC

Article

Structure and Luminescence Studies of Salts of the Helical Dication, $[Au_2(\mu\text{-bis(diphenylphosphine)ethane})_2]^{2+}$ and Comparison with Salts of $[Au_2(\mu\text{-bis(diphenylphosphine)propane})_2]^{2+}$

Sarah Costa, Daniel T. Walters, Lauren E. McNamara, Marilyn M. Olmstead, James C. Fettinger, and Alan. L. Balch*

Cite This: *Inorg. Chem.* 2023, 62, 15902−15911

Read Online

ACCESS | Metrics & More | Article Recommendations | Supporting Information

ABSTRACT: Six salts ($[Au_2(\mu\text{-dppe})_2](BF_4)_2\cdot CHCl_3$, $[Au_2(\mu\text{-dppe})_2](BF_4)_2\cdot 1,2\text{-}Cl_2C_2H_4$, $[Au_2(\mu\text{-dppe})_2](PF_6)_2\cdot CHCl_3$, $[Au_2(\mu\text{-dppe})_2](PF_6)_2$, $[Au_2(\mu\text{-dppe})_2](SbF_6)_2$, and $[Au_2(\mu\text{-dppe})_2](OTf)_2\cdot 2CHCl_3$), (dppe is bis(diphenylphosphine)ethane) containing the dication, $[Au_2(\mu\text{-dppe})_2]^{2+}$, have been prepared and structurally characterized by single-crystal X-ray crystallography. Unlike the three-coordinate dppe-bridged dimers, $Au_2X_2(\mu\text{-dppe})_2$ (X = Br, I), which show considerable variation in the distance between the gold(I) ions over the range 3.0995(10) to 3.8479(3) Å in various solvates, the structure of the helical dication, $[Au_2(\mu\text{-dppe})_2]$, in the new salts is remarkably consistent with the Au···Au separation falling in the narrow range 2.8787(9) to 2.9593(5) Å. In the solid state, the six crystals display a green luminescence both at room temperature and at 77 K, which has been assigned as phosphorescence. However, solutions of the dication are not luminescent. Salts containing the analogous dication $[Au_2(\mu\text{-dppp})_2](PF_6)_2$ (dppp is bis(diphenylphosphine)propane) have been prepared to determine whether the longer bridging ligand might also twist into a helical shape. These salts include $[Au_2(\mu\text{-dppp})_2](OTf)_2$ (OTf is triflate) and three crystalline forms of $[Au_2(\mu\text{-dppp})_2](PF_6)_2$: the solvate $[Au_2(\mu\text{-dppp})_2](PF_6)_2\cdot(CHCl_3)$ and two polymorphs of the unsolvated salt. None of these crystals are luminescent, but all contain a similar dication, $[Au_2(\mu\text{-dppp})_2]^{2+}$, that contains two nearly parallel, linear P−Au−P groups and a long separation between the gold ions that varies from 5.3409(4) to 5.6613(6)Å.

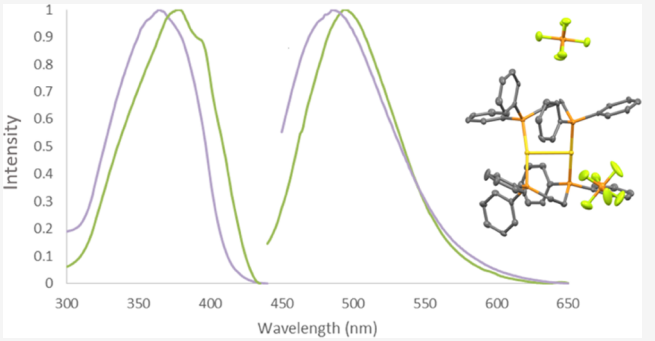

INTRODUCTION

Many gold(I) complexes display interesting luminescent properties that make them promising candidates for applications in sensing and electro-optic devices.[1−6] For example, three-coordinate, planar gold(I) complexes are generally luminescent both in the solid state and in solution.[7−11] For such trigonal planar complexes, the excitation process involves a transition from the filled, in-plane $d_{x^2-y^2}$,d_{xy} gold orbitals to an empty orbital that may be a ligand-based orbital or a p_z gold orbital and may cause significant distortion of the excited state.[10,11]

On the other hand, two-coordinate linear gold(I) complexes are frequently nonemissive but can become emissive through aurophilic interactions with another gold(I) center.[1,12−15] For example, salts containing the cations, $[(cyclohexylNC)_2Au]^+$, exhibit no luminescence when the cations are isolated from one another but show vibrant emission when aggregation occurs due to the formation of close contacts between the gold(I) ions.[16−20]

Prior work has demonstrated that planar, three-coordinate, gold(I) complexes bridged by bis(diphenylphosphine)ethane, (dppe), ligands show remarkable flexibility that is reflected in the Au···Au distance and in the luminescence of the complexes. For example, dimeric $Au_2(\mu\text{-dppe})_2Br_2$ crystallizes as a variety of different solvates in which the Au···Au separations range from 3.0995(10) to 3.8479(3)Å.[21] Figure 1 shows the structure of one such solvate, $Au_2(\mu\text{-dppe})_2Br_2\cdot 2(OSMe_2)$, which has the longest Au···Au separation, 3.8479(3) Å. The luminescence for different solvates of $Au_2(\mu\text{-dppe})_2Br_2$ varies. Crystals with Au···Au separations longer than 3.5 Å display orange luminescence, while those with Au···Au separations shorter than 3.5 Å produce green luminescence. While the presence of different solvate molecules in these crystals alters

Received: June 14, 2023
Published: September 18, 2023

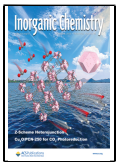

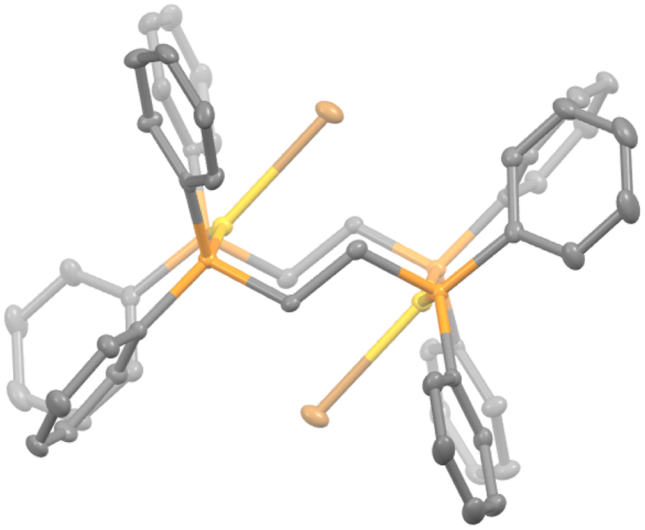

Figure 1. Structure of the centrosymmetric dimer, $Au_2(\mu\text{-dppe})_2Br_2$, in crystalline $Au_2(\mu\text{-dppe})_2Br_2{\cdot}2(OSMe_2)$ where the Au···Au separation is 3.8479(3) Å drawn with thermal contours at the 30% probability level. For clarity, hydrogen atoms and solvate molecules have been omitted. Color scheme: gold, yellow; phosphorus, orange; bromine, brown; carbon, gray.

the molecular packing, no direct interactions of the solvate molecules with the gold ions have been identified.

The related three-coordinate dimer, $Au_2(\mu\text{-dppe})_2I_2$, crystallizes from acetone solution as two polymorphs that also show flexibility of the bridging ligand. Crystals of α-$Au_2(\mu\text{-dppe})_2I_2{\cdot}2OCMe_2$ exhibit orange emission and an Au···Au distance of 3.6720(2) Å, while colorless crystals of β-$Au_2(\mu\text{-dppe})_2I_2{\cdot}2OCMe_2$ (2) display a green emission and a shorter Au···Au distance of 3.3955(2) Å.[22]

Most other two-coordinate gold(I) complexes lack aurophilic interactions and luminescence. However, based on the previous work, we became interested in examining the luminescence and structure of the dimeric dication $[Au_2(\mu\text{-dppe})_2]^{2+}$.[23,24] Peringer and co-workers examined the structure of $[Au_2(\mu\text{-dppe})_2](OTf)_2{\cdot}2CH_3OH$ and observed that it had a helical structure with a short Au···Au distance of 2.9594(10) Å and two distinct environments for the phosphorus atoms.[25] Nevertheless, in solution, only a single ^{31}P NMR resonance was detected, which the authors suggested came from rapid exchange. Awuah and co-workers found a similar structure for the dication in another salt, $[Au_2(\mu\text{-dppe})_2](ClO_4)_2{\cdot}CH_3CN$.[26] However, they also reported a computed structure at the B3LYP level that produced a more symmetrical, nonhelical structure with an Au···Au separation of 4.494 Å. Since solvate molecules and poorly coordinated anions can influence the structures of gold(I) complexes,[27−30] we have prepared and examined several other salts containing the dimeric dication, $[Au_2(\mu\text{-dppe})_2]^{2+}$, to examine their luminescence and the possibility that the cation structure might be flexible and readily altered. We have also prepared and examined the structure of the related dication, $[Au_2(\mu\text{-dppp})_2]^{2+}$ (dppp is bis(diphenylphosphine)propane), with a longer bridging diphosphine ligand in order to see how the longer bridge affects the structure and luminescence. In related cases, longer bridging diphosphines tend to create longer separations between gold(I) centers in dinuclear complexes.[31,32] It is also interesting to note that with only one bridging dppe ligand, the two-coordinate complex, AuCl(μ-dppp)AuCl, lacks intramolecular aurophilic interactions but dimerizes via two intermolecular aurophilic interactions in the solid state.[33,34]

RESULTS AND DISCUSSION

Preparation of Salts of $[Au_2(\mu\text{-dppe})_2]^{2+}$. Salts containing $[Au_2(\mu\text{-dppe})_2]^{2+}$ were obtained by mixing dichloromethane solutions of equimolar amounts of thtAuCl and dppe followed by the addition of the appropriate anion from sodium tetrafluoroborate, ammonium hexafluorophosphate, sodium hexafluorostibonate, or potassium triflate in a mixture of dichloromethane and methanol. The resulting solutions were evaporated to dryness, and the resulting solids were treated with dichloromethane to extract the gold salt. The dichloromethane solution was evaporated to dryness. Colorless crystals of $[Au_2(\mu\text{-dppe})_2](BF_4)_2{\cdot}CHCl_3$, $[Au_2(\mu\text{-dppe})_2](BF_4)_2{\cdot}1,2\text{-}Cl_2C_2H_4$, $[Au_2(\mu\text{-dppe})_2](PF_6)_2{\cdot}CHCl_3$, $[Au_2(\mu\text{-dppe})_2](SbF_6)_2$, and $[Au_2(\mu\text{-dppe})_2](OTf)_2{\cdot}2(CHCl_3)$, each with a green luminescence, were grown by slow diffusion of a mixture of diethyl ether or toluene into a chloroform or 1,2-dichloroethane solution of the salt.

Crystallographic Characterization of Salts Containing $[Au_2(\mu\text{-dppe})_2]^{2+}$. The structure of the dication, $[Au_2(\mu\text{-dppe})_2]^{2+}$, changes only slightly in the six different crystalline salts examined here and is similar to that found earlier in $[Au_2(\mu\text{-dppe})_2](OTf)_2{\cdot}2CH_3OH$ and $[Au_2(\mu\text{-dppe})_2](ClO_4)_2{\cdot}CH_3CN$.[25,26] Figure 2 shows two views of the dication in crystals of $[Au_2(\mu\text{-dppe})_2](BF_4)_2{\cdot}(CHCl_3)$. The view labeled B of this figure shows that the cation has a helical geometry with the bridging diphosphine ligands twisting about the two gold ions. These diphosphine ligands are arranged so that two of the eight phenyl rings extend outward at one end of the dication on the left side of Figure 2A, while four of the phenyl groups protrude outwardly at the opposite end of the dication on the right side of Figure 2A. In the salts reported here, individual dications are chiral due to their helical shape. However, these salts form in the centrosymmetric space groups, $P2_1/c$ or $P\bar{1}$, and consequently, each crystal contains a racemate of the dications.

Figure 3 shows the numbering scheme of the dication. Table 1 presents bond distances, bond angles, and torsional angles for the dication in the different salts. Each gold ion is bound to two phosphorus atoms of the bridging dppe ligands and to the other gold ion. The Au···Au distance varies only slightly over the range, 2.8787(9) to 2.9593(5)Å. In contrast, the three-coordinate, centrosymmetric dimer, $Au_2(\mu\text{-dppe})_2Br_2$, has a large variation in the Au···Au separation from 3.0943(2) to 3.8479(3)Å in different solvated crystals.[21,22] In $[Au_2(\mu\text{-dppe})_2]^{2+}$, the P1−Au1−P4 bond angles range from 164.82(3) to 171.37(3)°, while the P2−Au2−P3 bond angles, which range from 174.14(3) to 179.21(7)°, are more nearly linear. The Au2 center is consistently near the anions with two phenyl rings pointed away from the cation. In comparison to these bond angles, the torsional angles, P2−Au2···Au1−P1 and P3−Au2···Au1−P4, are nearly equal in the hexafluorophosphate, hexafluoroantimonate, and triflate salts. These torsional angles differ significantly only in the two solvated forms of the smallest anion, the tetrafluoroborate salts.

Spectroscopic Properties of the Dication, $[Au_2(\mu\text{-dppe})_2]^{2+}$. Each of the six salts reported here exhibits green luminescence in the solid state at room temperature. The excitation and emission spectra of crystals of $[Au_2(\mu\text{-dppe})_2](BF_4)_2{\cdot}CHCl_3$ are shown in Figure 4. The excitation

https://doi.org/10.1021/acs.inorgchem.3c01961
Inorg. Chem. 2023, 62, 15902−15911

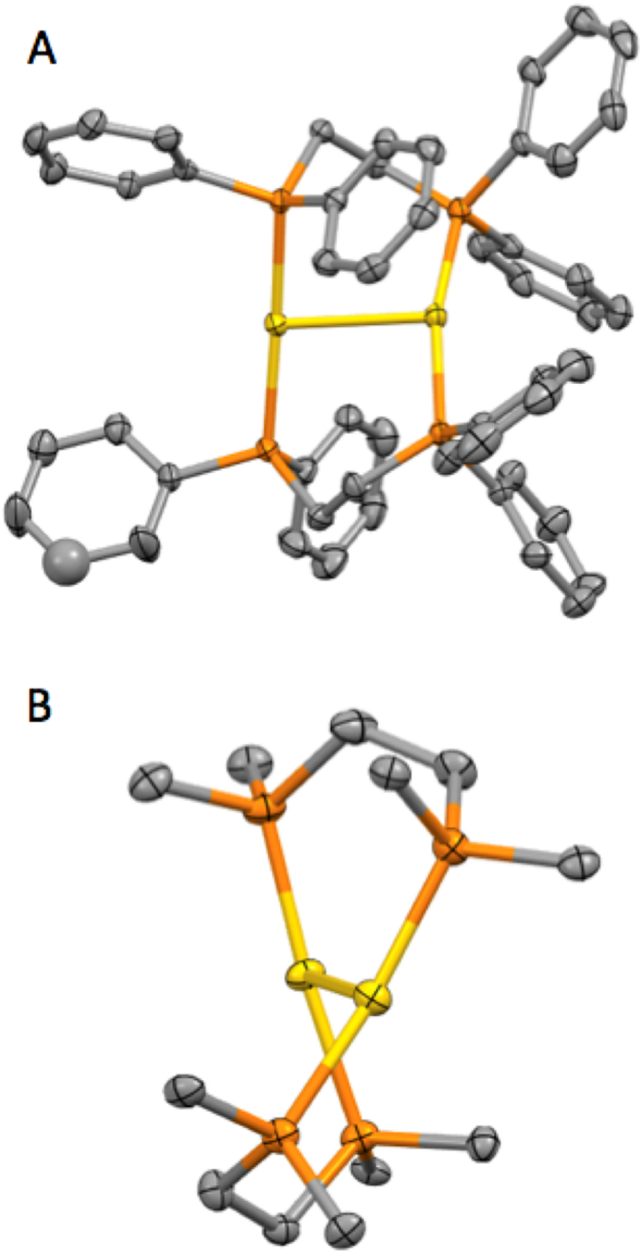

Figure 2. Two views of the structure of the dication $[Au_2(\mu\text{-dppe})_2]^{2+}$, in crystalline $[Au_2(\mu\text{-dppe})_2](BF_4)_2\cdot(CHCl_3)$ drawn with thermal contours at the 50% probability level. In (A) the phenyl rings are shown, but hydrogen atoms are omitted. In (B) only the ipso carbon atoms of each phenyl ring are shown for clarity. Color scheme: gold, yellow; phosphorus, orange; carbon, gray.

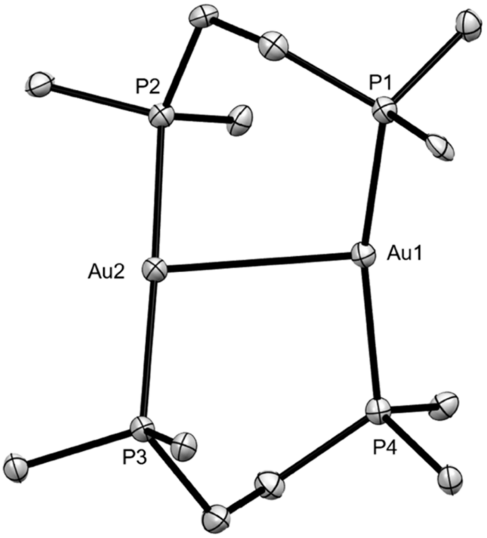

Figure 3. Numbering scheme for the dication $[Au_2(\mu\text{-dppe})_2]^{2+}$. Only the ipso carbon atom of each phenyl ring is shown for clarity. Anions and solvate molecules are not shown.

and emission spectra of the other crystals are similar and are shown in the Supporting Information. The excitation and emission wavelengths and lifetimes for these salts are given in Table 2. Based on the large Stokes shifts in these spectra and the microsecond lifetimes, it appears that the emissions of these salts are due to phosphorescence.

The UV spectrum of an acetonitrile solution of $[Au_2(\mu\text{-dppe})_2](PF_6)_2$ is shown in Figure 5. Notice that there is no significant absorption at 365 nm, where the crystalline forms of this cation display their excitation maxima. This observation suggests that the structure of $[Au_2(\mu\text{-dppe})_2]^{2+}$ in solution differs from the structure found in the solid state. It is possible that this dication in solution has a structure like that calculated by Awuah and co-workers with a long separation between the gold(I) ions and no significant aurophilic interaction, which is why there is no luminescence.[26]

At room temperature, colorless solutions of salts containing the dication, $[Au_2(\mu\text{-dppe})_2]^{2+}$, are not emissive. However, upon freezing in liquid nitrogen, these solutions become luminescent. Relevant spectra for solid $[Au_2(\mu\text{-dppe})_2](PF_6)_2$ and frozen solutions of this salt in a variety of solvents are shown in Figure 6. As the spectra show, there is a dependence of the excitation and emission wavelengths on the nature of the frozen solvent involved. Solvation effects, particularly in the vicinity of the gold ions, are the likely cause of the minor differences in these spectra in Figure 6. There is a precedent for such behavior, the dimeric dication, $[Au_2(\mu\text{-dpae})_2]^{2+}$ (dpae is 1,2-bis(diphenylarsino)ethane), has a helical structure analogous to that of $[Au_2(\mu\text{-dppe})_2]^{2+}$.[35] Over time, crystals of the disolvate $[Au_2(\mu\text{-dpae})_2](AsF_6)_2\cdot 2(CHCl_3)$ lose chloroform and are converted into the monosolvate, $[Au_2(\mu\text{-dpae})_2](AsF_6)_2\cdot(CHCl_3)$. This process is accompanied by a change in luminescence and a change in the surroundings of one of the gold ions in the dication.

The $^{31}P\{^1H\}$ NMR spectrum of $[Au_2(\mu\text{-dppe})_2](BF_4)_2$ in chloroform-*d* solution shows a single resonance at 38.4 ppm at 290 K. Cooling the solution results only in a slight downfield shift to 38.2 ppm at 273 K, 38.2 ppm at 263 K, and 38.1 ppm at 253 K. These results are consistent with the data reported by Peringer and co-workers, who observed only a single $^{31}P\{^1H\}$ NMR resonance at all temperatures for a solution of $[Au_2(\mu\text{-dppe})_2](OTf)_2\cdot 2CH_3OH$.[25] The observation of only a single $^{31}P\{^1H\}$ resonance could be explained by either rapid exchange of the phosphorus atoms between the two different environments seen in the crystal or by the existence of a more symmetrical, nonhelical structure like that computed by Awuah and co-workers in solution.[26]

Infrared spectra are reported for these salts in the Experimental Section. These spectra are dominated by vibrations of the diphosphine ligand, but there are also characteristic vibrational bands due to the individual anions that distinguish each spectrum.

https://doi.org/10.1021/acs.inorgchem.3c01961
Inorg. Chem. 2023, 62, 15902−15911

Table 1. Selected Bond Distances and Angles for $[Au_2(\mu\text{-dppe})_2]^{2+}$

complex	$[Au_2(\mu\text{-dppe})_2](BF_4)_2{\cdot}CHCl_3$	$[Au_2(\mu\text{-dppe})_2](BF_4)_2{\cdot}1,2\text{-}Cl_2C_2H_4$	$[Au_2(\mu\text{-dppe})_2](PF_6)_2{\cdot}CHCl_3$	$[Au_2(\mu\text{-dppe})_2](PF_6)_2$	$[Au_2(\mu\text{-dppe})_2](SbF_6)_2$	$[Au_2(\mu\text{-dppe})_2](OTf)_2{\cdot}2CHCl_3$
Distances (Å)						
Au−Au	2.8954(4)	2.8787(9)	2.9414(5)	2.9329(5)	2.9460(4)	2.9593(5)
Au1−P1	2.302(2)	2.301(1)	2.3087(9)	2.319(2)	2.305(1)	2.3146(9)
Au1−P4	2.302(2)	2.299(1)	2.3060(7)	2.313(2)	2.307(1)	2.312(1)
Au2−P2	2.325(1)	2.3133(9)	2.3056(9)	2.299(2)	2.307(1)	2.308(1)
Au2−P3	2.316(2)	2.3254(9)	2.3157(7)	2.313(2)	2.304(1)	2.312(1)
Angles (deg)						
P1−Au1−P4	164.82(6)	164.82	166.09(3)	170.88(7)	171.32(5)	171.37(3)
P2−Au2−P3	174.61(6)	174.14	177.86(3)	179.21(7)	176.92(5)	176.17(3)
Torsional Angles (deg)						
P2−Au2···Au1−P1	54.79(6)	38.56(3)	41.81(3)	42.73(7)	47.76(5)	47.06(3)
P3−Au2···Au1−P4	39.16(6)	54.65(3)	45.32(3)	45.40(7)	46.64(5)	47.23(3)

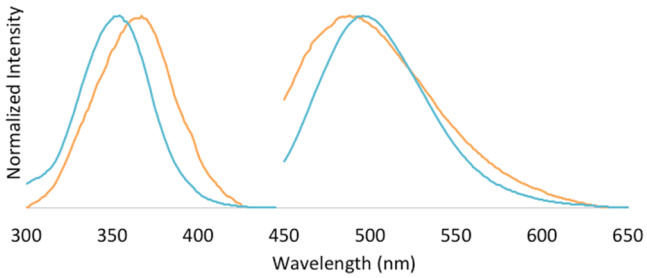

Figure 4. Excitation and emission spectra of crystals of $[Au_2(\mu\text{-dppe})_2](BF_4)_2{\cdot}CHCl_3$ at room temperature are shown in blue (emission obtained with excitation at 367 nm, excitation obtained for emission at 493 nm) and at 77 K in orange (emission obtained with excitation at 354 nm, excitation obtained for emission at 488 nm).

$[Au_2(\mu\text{-dppp})_2]^{2+}$. Salts containing $[Au_2(\mu\text{-dppp})_2]^{2+}$ were obtained by mixing dichloromethane solutions of equimolar amounts of thtAuCl and dppe, followed by the addition of ammonium hexafluorophosphate or potassium triflate in a mixture of dichloromethane and methanol as described for salts of $[Au_2(\mu\text{-dppe})_2]^{2+}$. Three crystalline forms of $[Au_2(\mu\text{-dppp})_2](PF_6)_2$ and $[Au_2(\mu\text{-dppp})_2](OTf)_2$ were grown concomitantly by diffusion of diethyl ether into a chloroform solution of the salt.

Structural Characterization of $[Au_2(\mu\text{-dppp})_2](PF_6)_2$ and $[Au_2(\mu\text{-dppp})_2](OTf)_2$. Three colorless crystalline salts containing the dication $[Au_2(\mu\text{-dppp})_2]^{2+}$ with hexafluorophosphate as the counterion have been obtained: the solvate $[Au_2(\mu\text{-dppp})_2](PF_6)_2{\cdot}(CHCl_3)$ and two polymorphs (designated as the α and β forms) of the unsolvated salt.

The structure of the dication, $[Au_2(\mu\text{-dppp})_2]^{2+}$, in the solvate $[Au_2(\mu\text{-dppp})_2](PF_6)_2{\cdot}(CHCl_3)$ is shown in part A of Figure 7, where its structure is compared with that of the α−polymorph $[Au_2(\mu\text{-dppp})_2](PF_6)_2$ in part B. The dication in the solvate $[Au_2(\mu\text{-dppp})_2](PF_6)_2{\cdot}(CHCl_3)$ has no crystallographic symmetry, while the dication in the α−polymorph $[Au_2(\mu\text{-dppp})_2](PF_6)_2$ is centrosymmetric. Figure 8 offers another comparison of the structure of the dication in $[Au_2(\mu\text{-dppp})_2](PF_6)_2{\cdot}(CHCl_3)$ with the structure of the dication in the centrosymmetric α−polymorph of $[Au_2(\mu\text{-dppp})_2](PF_6)_2$. In Figure 8, these dications are viewed down the P−Au−P axes of each dication. The structure of the dication in the β polymorph of $[Au_2(\mu\text{-dppp})_2](PF_6)_2$ is also centrosymmetric, with a structure similar to that of the α polymorph. Likewise, the dication in $[Au_2(\mu\text{-dppp})_2](OTf)_2$ is also centrosymmetric and has a structure similar to that of the centrosymmetric dimer shown in Figures 7 and 8. In all these structures, the P−Au−P units are nearly linear and parallel to one another with a rather long separation of the two gold ions, which ranges from 5.3409(4) to 5.6613(6)Å. Comparative structural data are given in Table 3.

Figure 7 also shows the structure of the related three-coordinate dimer, $Au_2I_2(\mu\text{-dppp})_2$, whose structure was reported earlier.[32] $Au_2I_2(\mu\text{-dppp})_2$ also has a centrosymmetric structure, with the two gold ions widely separated by 5.067(2) Å. Each gold ion is coordinated to two phosphorus atoms and an iodide ion. Since the complex contains three-coordinate gold(I), the P−Au−P angle (152.88(5)°) is far from linear.

Spectroscopic Properties of the Dication, $[Au_2(\mu\text{-dppp})_2]^{2+}$. The $^{31}P\{^1H\}$ NMR spectra of samples of $[Au_2(\mu\text{-dppp})_2](PF_6)_2$ and $[Au_2(\mu\text{-dppp})_2](OTf)_2$ showed a single

https://doi.org/10.1021/acs.inorgchem.3c01961
Inorg. Chem. 2023, 62, 15902−15911

Table 2. Data for Excitation and Emission of Salts Containing $[Au_2(\mu\text{-dppe})_2]^{2+}$

			298 K			77K		
crystal composition	Au−Au bond distance (Å)	visual color	emission (nm)	lifetime (ms)	excitation (nm)	emission (nm)	lifetime (ms)	excitation (nm)
$[Au_2(\mu\text{-dppe})_2](BF_4)_2{\cdot}CHCl_3$	2.878(6)	green	484	32	367	486	33	354
$[Au_2(\mu\text{-dppe})_2](BF_4)_2{\cdot}1,2\text{-}Cl_2C_2H_4$	2.878(6)	green	484	32	355	486	33	348
$[Au_2(\mu\text{-dppe})_2](PF_6)_2{\cdot}CHCl_3$	2.941(5)	green	474	32	378	485	34	364
$[Au_2(\mu\text{-dppe})_2](PF_6)_2$	2.9329(5)	green	494		374	495		350
$[Au_2(\mu\text{-dppe})_2](SbF_6)_2$	2.95(2)	green	494	11	361	501	34	357
$[Au_2(\mu\text{-dppe})_2]OTf_2CHCl_3$	2.959(4)	green	491	32	364	491	32	358

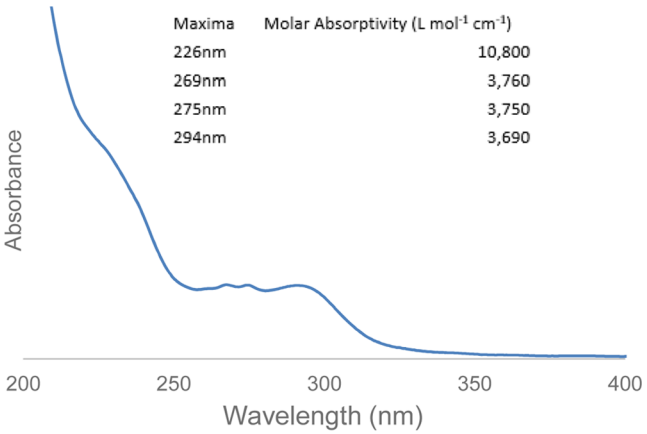

Figure 5. UV spectrum of $[Au_2(\mu\text{-dppe})_2](PF_6)_2$ in an acetonitrile solution at room temperature.

resonance at 41.5 ppm at room temperature. None of the salts containing the dication $[Au_2(\mu\text{-dppp})_2]^{2+}$ showed any luminescence at 77 K or at room temperature. Solutions of these salts were not luminescent. The lack of luminescence is consistent with the large separation between the gold ions in these dimers, which prevents aurophilic interactions. In contrast, the neutral binuclear complex, $Au_2I_2(\mu\text{-dppp})_2$, whose structure is shown in Figure 7, is luminescent at room temperature with λ_{exc} = 350 nm and λ_{em} = 420 nm as reported previously.[32] The luminescence of the dimer of $[Au_2(\mu\text{-dppp})_2]^{2+}$ is expected as it is seen in the three-coordinate gold complexes.

CONCLUSIONS

While the three-coordinate dppe-bridged dimers, $Au_2X_2(\mu\text{-dppe})_2$ (X = Br, I), show considerable variation in the distance between the gold(I) ions over the range of 3.8479(3)−3.0995(10) Å in various crystalline solvates, the structure of the dication, $[Au_2(\mu\text{-dppe})_2]^{2+}$, in the new salts reported here is remarkably consistent with a helical structure that brings the Au···Au separation into the narrow range 2.8787(9) to 2.9593(5) Å. In other words, the anion or the solvate molecules produce only very minor changes in the Au···Au separation. With the two-coordinate gold ions experiencing aurophilic interactions in these salts, each emits a green luminescence at room temperature and at 77 K. However, solutions of the dication are nonluminescent, possibly due to a change in structure with an increase in the separation between the gold(I) ions.

The gold(I) ions in the dication $[Au_2(\mu\text{-dppp})_2]^{2+}$ are widely separated in the various crystals examined here. The longer dppp bridging ligand does not participate in helical

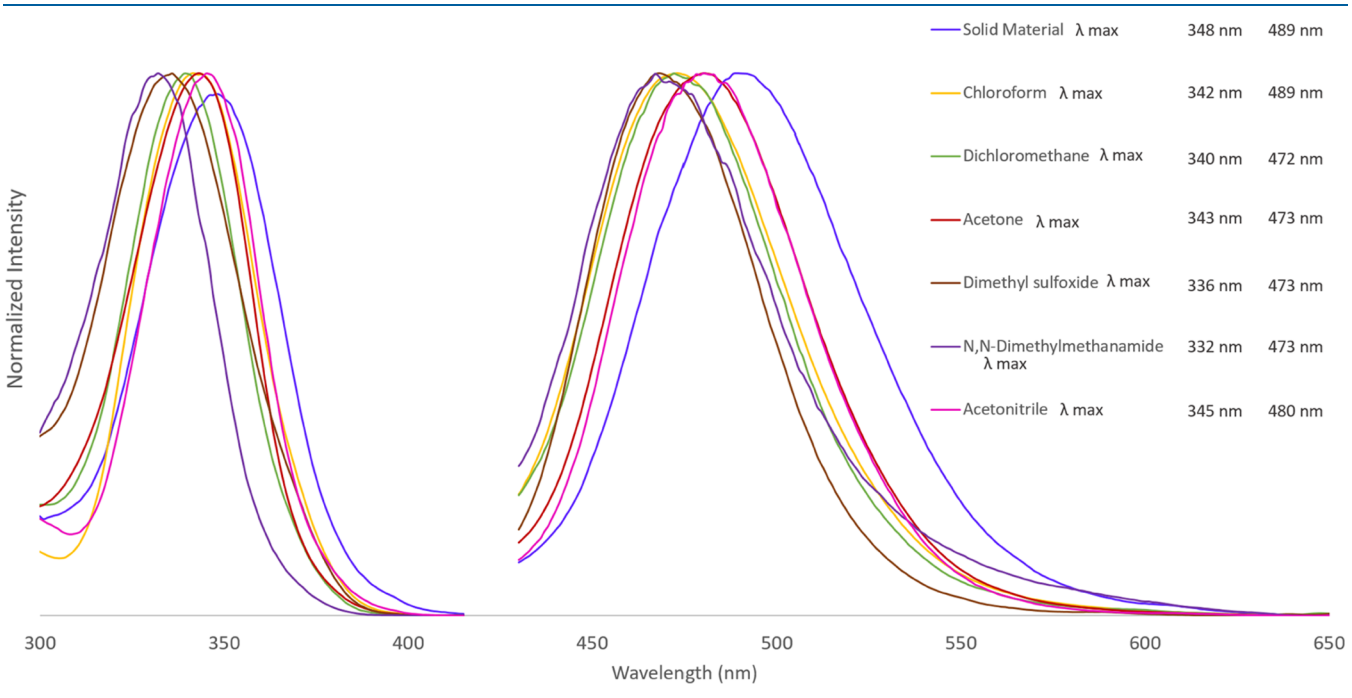

Figure 6. Excitation (left) and emission (right) spectra of $[Au_2(\mu\text{-dppe})_2](PF_6)_2$ as a solid and in various frozen solutions at 77 K.

https://doi.org/10.1021/acs.inorgchem.3c01961
Inorg. Chem. 2023, 62, 15902−15911

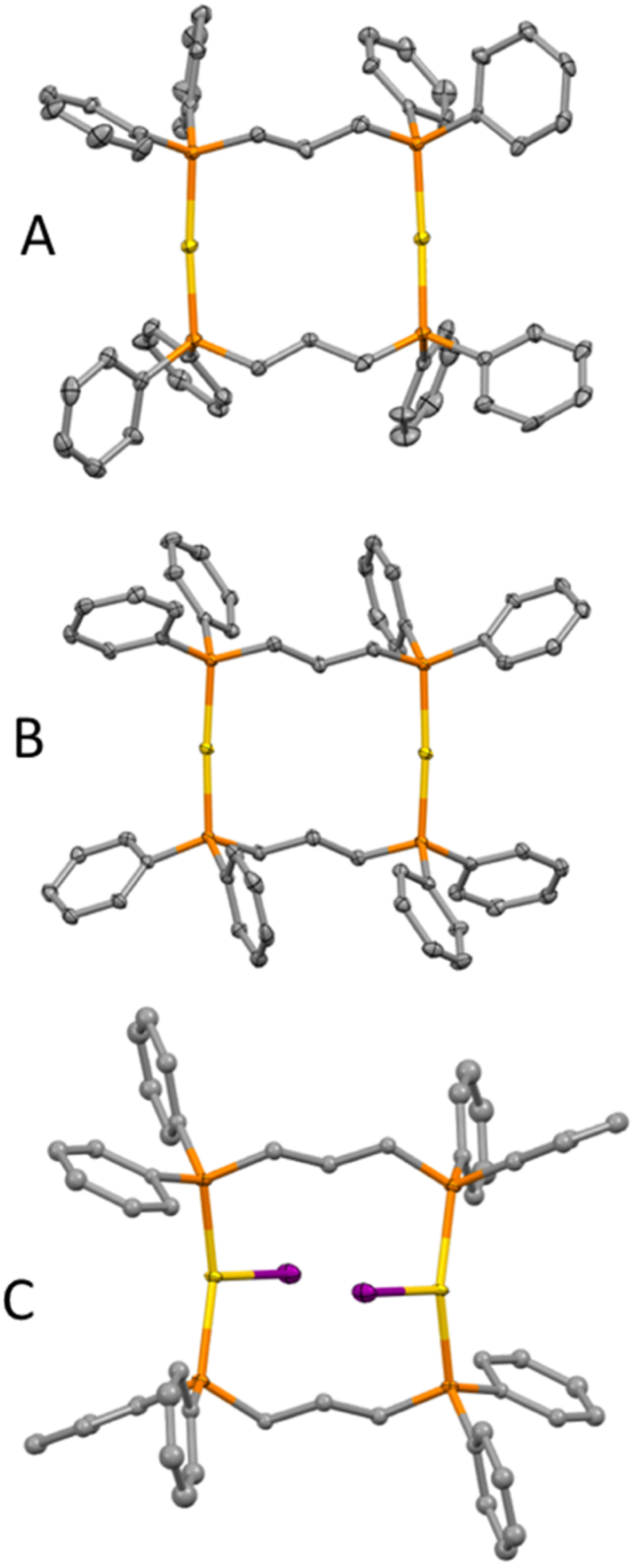

Figure 7. (A) the structure of the dication, $[Au_2(\mu\text{-dppp})_2]^{2+}$, in crystalline $[Au_2(\mu\text{-dppp})_2](PF_6)_2{\cdot}CHCl_3$; (B) the structure of the centrosymmetric dication, $[Au_2(\mu\text{-dppp})_2]^{2+}$, in the α polymorph of $[Au_2(\mu\text{-dppp})_2](PF_6)_2$; and (C) the structure of centrosymmetric $Au_2I_2(\mu\text{-dppp})_2$ drawn from coordinates from ref 32 with all thermal contours at the 50% probability level. Color scheme: gold, yellow; phosphorus, orange; iodine, violet; carbon, gray.

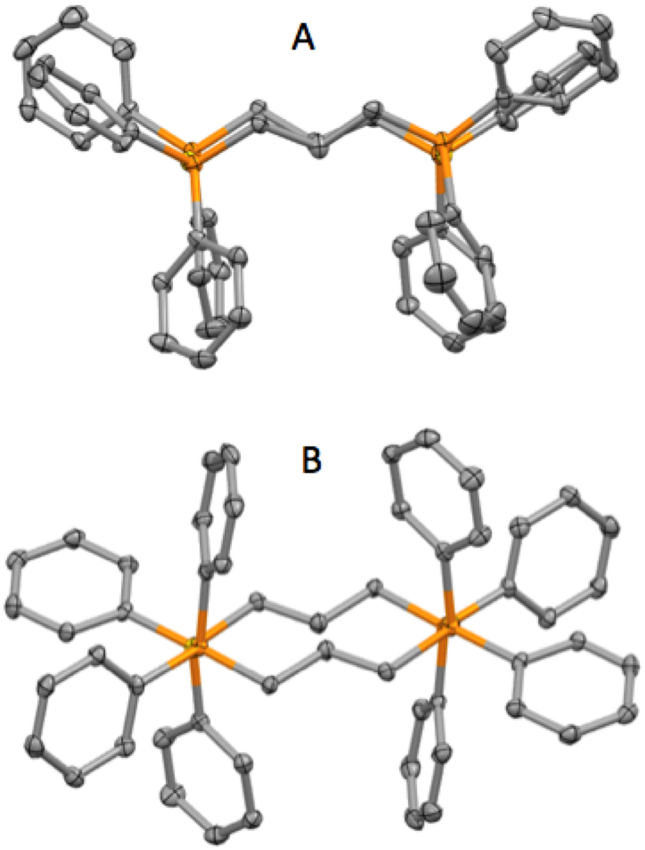

Figure 8. Views down the P−Au−P bonds of: (A) the dication, $[Au_2(\mu\text{-dppp})_2]^{2+}$, in crystalline $[Au_2(\mu\text{-dppp})_2](PF_6)_2{\cdot}CHCl_3$; (B) the centrosymmetric dication, $[Au_2(\mu\text{-dppp})_2]^{2+}$, in the α polymorph of $[Au_2(\mu\text{-dppp})_2](PF_6)_2$. Color scheme: gold, yellow; phosphorus, orange; carbon, gray.

twisting that is characteristic for the dication $[Au_2(\mu\text{-dppe})_2]^{2+}$ and does not allow the gold(I) ions to engage in aurophilic interactions. Other cases are known where bridging diphosphines with three or more methylene groups between the phosphorus atoms keep metal centers apart and restrict metallophilic interactions.[31,32,36]

EXPERIMENTAL SECTION

Preparation of Compounds. Methanol, toluene, and dichloromethane were purchased from Sigma-Aldrich Co., LLC. Chloroauric acid was purchased from Strem Chemicals, Inc. Ammonium hexafluorophosphate was purchased from Alfa Aesar, Inc. Solids were used as received. Solvents were used as received, and all reactions were conducted on the benchtop open to the atmosphere.

Preparation of $[Au_2(\mu\text{-dppe})_2](BF_4)_2{\cdot}CHCl_3$. A 82.5 mg (0.207 mmol) portion of dppe was dissolved in 7 mL of dichloromethane, and an equivalent amount of thtAuCl (66.4 mg, 0.207 mmol) that had been dissolved in 4 mL of dichloromethane was added to the dppe solution. This solution was stirred for about 10 min followed by the addition of $NaBF_4$ (228.5 mg, 2.07 mmol) that was dissolved in 6 mL of dichloromethane and 2 mL of methanol. The colorless solution was then stirred over a 24-h period. To remove the excess salt, the crude product was vacuum-dried, and the resulting solid was dissolved in a minimum amount of dichloromethane. The colorless solution was filtered using a filter pipet, and the filtrate was evaporated to dryness. A crude yield of 119.5 mg (85%) was obtained. The dried crude product was dissolved in chloroform and filtered. This solution was placed at the bottom of an outer diameter of 5 mm diameter glass tube, and antisolvent of diethyl ether or toluene was layered above it.

https://doi.org/10.1021/acs.inorgchem.3c01961
Inorg. Chem. 2023, 62, 15902−15911

Table 3. Selected Bond Distances and Angles for $[Au_2(\mu\text{-dppp})_2]^{2+}$

complex	$[Au_2(\mu\text{-dppp})_2](PF_6)_2\cdot(CHCl_3)$	$\alpha\text{-}[Au_2(\mu\text{-dppp})_2](PF_6)_2$	$\beta\text{-}[Au_2(\mu\text{-dppp})_2](PF_6)_2$	$[Au_2(\mu\text{-dppp})_2](OTf)_2$
		distances (Å)		
Au−Au	5.6613(6)	5.6414(3)	5.3409(4)	5.602(1)
intraligand P···P	5.558(3)	5.483	5.5478(8)	
	5.505(3)			
Au1−P1	2.309(2)	2.3176(7)	2.3045(9)	2.310(2)
Au1−P4	2.311(2)	2.3189(7)	2.3086(9)	2.310(2)
Au2−P2	2.308(2)	2.3189(7)	2.3086(9)	2.310(2)
Au2−P3	2.307(2)	2.3176(7)	2.3045(9)	2.310(2)
		angles (deg)		
P1−Au1−P4	174.60(7)	175.95(3)	169.44(3)	178.4(5)
P2−Au2−P3	175.31(8)	175.95(3)	169.44(3)	178.4(5)
		torsional angles (deg)		
P2−Au2−Au1-P1	6.81(7)	1.04(3)	9.40(3)	0.00
P3−Au2−Au1-P4	6.17(7)	1.04(3)	9.40(3)	0.00

Colorless crystals with green luminescence grew over a two-week period.

Infrared spectra (cm^{-1}): 3051 (w), 3018 (w), 2965 (w), 1585 (w), 1486 (w), 1434 (m), 1404 (w), 1270 (m), 1248 (m), 1227(w), 1171 (w), 1132 (m), 1098 (s), 1025 (vs), 996 (m), 919 (w), 872 (w), 841 (w), 796 (w), 737 (s), 689 (vs), 630 (s), 570 (w), 514 (w), 477 (m), 422 (m). The peak at 1025 (vs) cm^{-1} correlates to the B−F stretch of the BF_4^- anion.

$^{31}P\{^1H\}$ Nuclear Magnetic Resonance (ppm): 38.4 ppm in chloroform-*d* at 290 K.

Preparation of $[Au_2(\mu\text{-dppe})_2](PF_6)_2$. This salt was obtained in 70% yield following the procedure used to prepare $[Au_2(\mu\text{-dppe})_2](BF_4)_2\cdot CHCl_3$ with the substitution of ammonium hexafluorophosphate for sodium tetrafluoroborate.

Infrared spectra (cm^{-1}): 3050 (w), 3018 (w), 2965 (w), 1479 (w), 1435 (m), 1399 (w), 1337 (w), 1303 (w), 1269 (w), 1184 (w), 1101(m), 1074 (w), 1030 (w), 994 (w), 828 (vs), 736 (m), 685 (s), 556 (m), 515 (s), 471 (m). The peaks at 828 (vs) and 556 (m) cm^{-1} correlate to the P−F stretch and bend of the PF_6^- anion.

$^{31}P\{^1H\}$ Nuclear Magnetic Resonance: 38.4 ppm in chloroform-*d* at 290 K.

^1H Nuclear Magnetic Resonance: complex multiplets for the aromatic resonances at 7.67, 7.65, 7.62, 7.60, 7.48, 7.46, and 7.43 ppm (40 protons); methylene resonance, quintet, 3.30 ppm (8 protons) chloroform-*d* at 290 K.

Preparation of $[Au_2(\mu\text{-dppe})_2](SbF_6)_2$. This salt was obtained in 6.8% yield following the procedure used to prepare $[Au_2(\mu\text{-dppe})_2](BF_4)_2\cdot CHCl_3$ with the substitution of sodium hexafluoroantimonate for sodium tetrafluoroborate.

Infrared (cm^{-1}): 3058 (w), 2973 (w), 1585 (w), 1483 (w), 1436 (s), 1407 (w), 1333 (w), 1307 (w), 1270 (w), 1189 (w), 1132 (w), 1099 (m), 1070 (w), 1023 (w), 999 (w), 874 (w), 840 (w), 798 (w), 739 (m), 718 (w), 690 (s), 650 (vs), 565 (w), 524 (s), 512 (s), 467 (m), 439 (w), 418 (w) 396(w). The peak at 690 (s) cm^{-1} correlates with the Sb−F stretch of the SbF_6^- anion.

Preparation of $[Au_2(\mu\text{-dppe})_2](OTf)_2\cdot 2(CHCl_3)$. This salt was obtained in 93% yield following the procedure used to prepare $[Au_2(\mu\text{-dppe})_2](BF_4)_2\cdot CHCl_3$ with the substitution of potassium triflate for sodium tetrafluoroborate.

Infrared spectrum (cm^{-1}): 3052 (w), 2971(w), 1579 (w), 1479 (w), 1433 (m), 1408 (w), 1337 (w), 1297 (w), 1265 (m), 1249 (m), 1222 (m), 1148 (m), 1101 (m), 1025 (m), 993 (w), 915 (w), 881 (w), 846 (w), 799 (w), 725 (m), 686 (s), 630 (w), 570 (w), 514 (s), 472 (m). The peaks at 1297 (w), 1265 (m), 1249 (m), 1222 (m), 1025 (m), and 630 (w) cm^{-1} correlate to the C−F and S−O stretch and bend of the OTf^- anion.

Preparation of $[Au_2(\mu\text{-dppp})_2](PF_6)_2$. A 68.5 mg (0.166 mmol) portion of dppp was dissolved in 7 mL of dichloromethane, and an equivalent quantity of thtAuCl (51.9 mg, 0.162 mmol) dissolved in 4 mL of dichloromethane was added to the dppp solution. This colorless solution was stirred for 10 min, followed by the addition of potassium hexafluorophosphate (350 mg, 1.90 mmol) that was dissolved in a 6 mL portion of dichloromethane and 2 mL of methanol. This mixture was then stirred over a 24-h period. To remove the excess salt, the crude product was evaporated to dryness. The resulting solid was dissolved in dichloromethane and filtered with a filter pipet. The dried, green, luminescent crude product (yield: 184 mg, 75%) was dissolved in chloroform. Slow diffusion of diethyl ether into the colorless chloroform solution produced colorless crystals that did not luminesce under UV light at 77 K or room temperature.

$^{31}P\{^1H\}$ Nuclear Magnetic Resonance (ppm): 41.5 ppm (cation) and −144.12(J_{PF}, 3.54) ppm (anion) in chloroform-*d*.

Infrared spectra (cm^{-1}): 3066 (w), 2913 (w), 2850 (w), 1573 (w), 1483 (w), 1436 (m), 1314 (w), 1191 (w), 1185 (w), 1105 (m), 1000 (w), 996 (w), 960 (m), 827 (s), 744 (m), 691 (m), 688 (m), 555 (m), 486 (m), 481 (m), 463 (m), 422 (w), 392 (w). The peaks at 827 (s) and 555 (m) cm^{-1} correlate to the P−F stretch and bend of the PF_6^- anion.

Preparation of $[Au_2(\mu\text{-dppp})_2](OTf)_2$. This salt was obtained in 52% yield following the procedure used to prepare $[Au_2(\mu\text{-dppp})_2](PF_6)_2$ with the substitution of potassium hexafluorophosphate for potassium triflate.

$^{31}P\{^1H\}$ Nuclear Magnetic Resonance (ppm): 41.5 ppm.

Infrared spectrum (cm^{-1}): 3050 (w), 2950 (w), 2920 (w), 2899 (w), 2853 (w), 1481 (m), 1436 (s), 1405 (w), 1381 (w), 1259 (s), 1221 (m), 1160 (m), 1102 (s), 1067 (w), 1026 (s), 997 (m), 967 (m), 939 (m), 835 (m), 798 (w), 742 (s), 690 (s), 635 (s). The peaks at 1259 (s), 1221 (m), 1160 (m), 1026 (m), and 635(s) cm^{-1} correlate to the C−F and S−O stretch and bend of the OTf^- anion.

$^{31}P\{^1H\}$ Nuclear Magnetic Resonance: 41.4 ppm in chloroform-*d* at 290 K.

^1H Nuclear Magnetic Resonance: complex multiplets for the aromatic resonances at 7.64, 7.54, 7.53, and 7.52 ppm (40 protons); methylene resonance, broad multiplet, 3.04 ppm (8 protons); and 2.16 broad multiplet, ppm (4 protons) in chloroform-*d* at 290 K.

X-ray Crystallography and Data Collection. Crystals were coated with hydrocarbon oil after being transferred with a covering of mother liquor to a microscope slide. Colorless crystals of $[Au_2(\mu\text{-dppe})_2](BF_4)_2\cdot CHCl_3$, $[Au_2(\mu\text{-dppe})_2](PF_6)_2\cdot 2CHCl_3$ $[Au_2(\mu\text{-dppe})_2](PF_6)_2$, $[Au_2(\mu\text{-dppe})_2](BF_4)_2\cdot 1,2\text{-}Cl_2C_2H_4$, $[Au_2(\mu\text{-dppe})_2(OTf)_2]\cdot 2(CHCl_3)$, $[Au_2(\mu\text{-dppp})_2](PF_6)_2\cdot(CHCl_3)$, $[Au_2(\mu\text{-dppp})_2](PF_6)_2$, $[Au_2(\mu\text{-dppp})_2](OTf)_2$, and were mounted under a nitrogen cold stream produced by an Oxford Cryostream low-temperature apparatus on the goniometer head of a Bruker D8 Venture Kappa DUO diffractometer equipped with Bruker Photon II CMOS detector and a Mo Kα microsource. A colorless parallelepiped of $Au_2(dppe)_2(SbF_6)_2$ was mounted in the 100 K nitrogen cold stream provided by a Cryo Industries low-temperature apparatus on the goniometer head of a Bruker APEX II sealed-tube diffractometer and CCD detector with the use of Mo Kα (λ = 0.71073 Å) radiation.

https://doi.org/10.1021/acs.inorgchem.3c01961
Inorg. Chem. 2023, 62, 15902−15911

Table 4. Crystal Data

	$[Au_2(\mu\text{-dppe})_2](BF_4)_2\cdot CHCl_3$	$[Au_2(\mu\text{-dppe})_2](BF_4)_2\cdot 1,2\text{-}Cl_2C_2H_4$	$[Au_2(\mu\text{-dppe})_2](PF_6)_2\cdot 2CHCl_3$	$[Au_2(\mu\text{-dppe})_2](PF_6)$
color/habit	colorless block	colorless block	colorless block	colorless block
chemical formula	$C_{53}H_{49}Au_2B_2\ Cl_3F_8P_4$	$C_{54}H_{52}Au_2B_2\ Cl_2F_8P_4$	$C_{54}H_{50}Au_2Cl_6\ F_{12}P_6$	$C_{52}H_{48}Au_2\ F_{12}P_6$
formula weight	1483.72	1463.29	1719.39	1480.65
crystal system	monoclinic	monoclinic	triclinic	monoclinic
space group	$P2_1/c$	$P2_1/c$	$P\bar{1}$	$P2_1/c$
a/Å	21.0445(9)	21.075(6)	12.3528(17)	11.2050(2)
b/Å	13.0917(6)	13.134(4)	12.4980(17)	25.1101(5)
c/Å	20.1991(9)	19.698(5)	22.069(3)	18.5313(4)
α/deg	90	90	101.917(3)	90
β/deg	107.382(3)	104.334(7)	91.887(3)	96.3980(10)
γ/deg	90	90	114.272(3)	90
V/Å^3	5310.9(4)	5282(2)	3012.4(7)	5181.47(18)
Z	4	4	2	4
T (K)	90(2)	100(2)	100(2)	90(2)
λ (Å)	0.71073	0.71073	0.71073	0.71073
ρ (g/cm^3)	1.856	1.840	1.896	1.898
μ (mm^{-1})	5.855	5.836	5.364	5.922
R_1 (obsd data)[a]	0.0439	0.0499	0.021	0.0425
wR_2 (all data, F_2 refinement)[b]	0.1408	0.0631	0.0371	0.1461

	$[Au_2(\mu\text{-dppe})_2]\ (OTf)_2\cdot 2(CHCl_3)$	$[Au_2(\mu\text{-dppe})_2]\ (SbF_6)_2$	$[Au_2(\mu\text{-dppp})_2]\ (PF_6)_2\cdot(CHCl_3)$
color/habit	colorless needle	colorless parallelepiped	colorless block
chemical formula	$C_{56}H_{50}Au_2Cl_6F_6\ O_6P_4S_4$	$C_{52}H_{48}Au_2\ F_{12}P_4Sb_2$	$C_{55}\ H_{54}\ Au_2\ Cl_3\ F_{12}\ P_6$
formula weight	3335.81	1662.25	1629.08
crystal system	monoclinic	monoclinic	orthorhombic
space group	$P2_1/c$	$P2_1/c$	$P2_12_12_1$
a/Å	11.5718(10)	11.3952(9)	12.2983(2)
b/Å	36.444(3)	36.836(3)	18.3220(4)
c/Å	14.6822(13)	14.4435(12)	26.5245(5)
α/deg	90	90	90
β/deg	106.807(2)	106.711(3)	90
γ/deg	90	90	90
V/Å^3	5927.3(9)	5806.7(8)	5976.8(2)
Z	2	4	4
T (K)	100(2)	100(2)	90
λ (Å)	0.71073	0.71073	0.71073
ρ (g/cm^3)	1.869	1.901	1.806
μ (mm^{-1})	5.394	6.14	5.272
R_1 (obsd data)[a]	0.0267	0.0394	0.0329
wR_2 (all data, F_2 refinement)[b]	0.0505	0.0984	0.1026

	$[Au_2(\mu\text{-dppp})_2]\ (PF_6)_2$ (α polymorph)	$[Au_2(\mu\text{-dppp})_2]\ (PF_6)_2$ (β- polymorph)	$[Au_2(\mu\text{-dppp})_2]\ (OTf)_2$
color/habit	colorless parallelepiped	colorless plate	colorless block
chemical formula	$C_{54}H_{52}Au_2F_{12}P_6$	$C_{54}H_{52}Au_2F_{12}P_6$	$C_{56}H_{52}Au_2P_4F_6O_6S_2$
formula weight	1508.16	1508.72	1516.91
crystal system	triclinic	triclinic	orthorhombic
space group	$P\bar{1}$	$P\bar{1}$	*Ibam*
a/Å	9.0514(2)	10.5733(5)	15.2016(11)
b/Å	11.8984(2)	11.8113(5)	17.0643(12)
c/Å	14.0805(2)	13.4238(8)	21.6296(16)
α/deg	69.2180(10)	64.005(2)	90
β/deg	74.1960(10)	71.710(3)	90
γ/deg	79.3420(10)	64.425(2)	90
V/Å^3	1357.58(4)	1343.04(12)	5610.8(7)
Z	1	1	4
T (K)	90(2)	90(2)	190(2)
λ (Å)	0.71073	0.71073	0.71073
ρ (g/cm^3)	1.882	1.865	1.796
μ (mm^{-1})	5.654	5.713	5.481
R_1 (obsd data)[a]	0.0177	0.0179	0.0242
wR_2 (all data, F_2 refinement)[b]	0.0635	0.0678	0.0631

[a] $R_1 = (\Sigma||F_o| - |F_c||)/\Sigma|F_o|$ [b] $wR_2 = ((\Sigma[w(F_{o2} - F_c^2)^2])/\Sigma[w(F_o^2)^2])^{1/2}$

https://doi.org/10.1021/acs.inorgchem.3c01961
Inorg. Chem. 2023, 62, 15902−15911

Crystal data are found in Table 4. A multiscan absorption correction was applied with the program SADABS.[37] The structures were solved by a dual space method, (SHELXT)[38] and refined by full-matrix least-squares on F^2 (SHELXL-2017).[39] CCDC 2269736−2269741, 2269727−2269729, and 2286100 contain the supplementary crystallographic data for this paper.

Physical Measurements. IR spectra were recorded on a Bruker α FT-IR spectrometer by using attenuated total reflectance (ATR). Fluorescence excitation and emission spectra were recorded on a Jobin−Yvon−Horiba Floromax-P luminescence spectrophotometer. UV−vis spectra were recorded on a Shimadzu UV-3600 spectrophotometer.

■ ASSOCIATED CONTENT

Supporting Information

The Supporting Information is available free of charge at https://pubs.acs.org/doi/10.1021/acs.inorgchem.3c01961.

Drawings of the structures of each salt that contains the dication, $[Au_2(\mu\text{-dppe})_2]^{2+}$ (PDF)

Accession Codes

CCDC 2269727−2269729, 2269736−2269741, and 2286100 contain the supplementary crystallographic data for this paper. These data can be obtained free of charge via www.ccdc.cam.ac.uk/data_request/cif, or by emailing data_request@ccdc.cam.ac.uk, or by contacting The Cambridge Crystallographic Data Centre, 12 Union Road, Cambridge CB2 1EZ, UK; fax: +44 1223 336033.

■ AUTHOR INFORMATION

Corresponding Author

Alan. L. Balch − *Department of Chemistry, University of California, Davis, Davis, California 05616, United States;* orcid.org/0000-0002-8813-6281; Email: albalch@ucdavis.edu

Authors

Sarah Costa − *Department of Chemistry, University of California, Davis, Davis, California 05616, United States*

Daniel T. Walters − *Department of Chemistry, University of California, Davis, Davis, California 05616, United States*

Lauren E. McNamara − *Department of Chemistry, University of California, Davis, Davis, California 05616, United States;* orcid.org/0000-0002-1169-8171

Marilyn M. Olmstead − *Department of Chemistry, University of California, Davis, Davis, California 05616, United States;* orcid.org/0000-0002-6160-1622

James C. Fettinger − *Department of Chemistry, University of California, Davis, Davis, California 05616, United States;* orcid.org/0000-0002-6428-4909

Complete contact information is available at: https://pubs.acs.org/10.1021/acs.inorgchem.3c01961

Author Contributions

S.C., D.T.W., and L.E.M. contributed to synthetic studies and crystal growth, S.C., D.T.W., and M.M.O. contributed to crystal data collection and analysis, S.C. and A.L.B. contributed to writing.

Notes

The authors declare no competing financial interest.

■ ACKNOWLEDGMENTS

The authors thank the National Science Foundation (Grant CHE-1807637) for partial support of this project, and Grant CHE-1531193 for the Dual source X-ray diffractometer.

■ REFERENCES

(1) Balch, A. L. Remarkable Luminescence Behaviors and Structural Variations of Two-Coordinate Gold(I) Complexes. *Struct. Bonding* **2007**, *123*, 1.

(2) He, X.; Yam, V. W.-W. Luminescent gold(I) complexes for chemosensing. *Coord. Chem. Rev.* **2011**, *255*, 2111−2123.

(3) Yam, V. W. W.; Cheng, E. C. C. Highlights on the recent advances in gold chemistry—a photophysical perspective. *Chem. Soc. Rev.* **2008**, *37*, 1806−1813.

(4) Tiekink, E. R. T.; Kang, J.-G. Luminescence properties of phosphinegold(I) halides and thiolates. *Coord. Chem. Rev.* **2009**, *253*, 1627−1648.

(5) Yam, V.W.-W.; Au, V. K.-M.; Leung, S. Y.-L. Light-Emitting Self-Assembled Materials Based on d^8 and d^{10} Transition Metal Complexes. *Chem. Rev.* **2015**, *115*, 7589−7728.

(6) Jin, M.; Hajime Ito, H. Solid-state luminescence of Au(I) complexes with external stimuli-responsive properties. *J. Photochem. Photobiol., C* **2022**, *51*, No. 100478.

(7) Ziolo, R. F.; Lipton, S.; Z Dori, Z. The Photoluminescence of Phosphine Complexes of d^{10} Metals. *J. Chem. Soc. D* **1970**, 1124−1125.

(8) McCleskey, T. M.; Gray, H. B. Emission Spectroscopic Properties of l,2-Bis(dicyclohexylphosphino)ethane Complexes of Gold(I). *Inorg. Chem.* **1992**, *31*, 1773−1774.

(9) King, C.; Khan, M. N. I.; Staples, R. J.; Fackler, J. P., Jr. Luminescent mononuclear gold(I) phosphines. *Inorg. Chem.* **1992**, *31*, 3236.

(10) Barakat, K. A.; Cundari, T. R.; Omary, M. A. Jahn−Teller Distortion in the Phosphorescent Excited State of Three-Coordinate Au(I) Phosphine Complexes. *J. Am. Chem. Soc.* **2003**, *125*, 14228−14229.

(11) Sinha, P.; Wilson, A. K.; Omary, M. A. Beyond a T-Shape. *J. Am. Chem. Soc.* **2005**, *127*, 12488−12489.

(12) Pyykkö, P.; Li, J.; Runeberg, N. Predicted ligand dependence of the Au (I)···Au (I) attraction in $(XAuPH_3)$. *Chem. Phys. Lett.* **1994**, *218*, 133−137.

(13) Pyykkö, P. Strong Closed-Shell Interactions in Inorganic Chemistry. *Chem. Rev.* **1997**, *97*, 597−636.

(14) Schmidbaur, H.; Schier, A. Aurophilic interactions as a subject of current research: an up-date. *Chem. Soc. Rev.* **2012**, *41*, 370−412.

(15) Mirzadeh, N.; Privér, S. H.; Blake, A. J.; Schmidbaur, H.; Bhargava, S. K. Innovative Molecular Design Strategies in Materials Science Following the Aurophilicity Concept. *Chem. Rev.* **2020**, *120*, 7551−7591.

(16) White-Morris, R. L.; Olmstead, M. M.; Balch, A. L. Aurophilic Interactions in Cationic Gold Complexes with Two Isocyanide Ligands. Polymorphic Yellow and Colorless Forms of $[(Cyclohexyl\ Isocyanide)_2Au^I](PF_6)$ with Distinct Luminescence. *J. Am. Chem. Soc.* **2003**, *125*, 1033−1040.

(17) Malwitz, M. A.; Lim, S. H.; White-Morris, R. L.; Pham, D. M.; Olmstead, M. M.; Balch, A. L. Crystallization and Interconversions of Vapor-Sensitive, Luminescent Polymorphs of $[(C_6H_{11}NC)_2Au^I](AsF_6)$ and $[(C_6H_{11}NC)_2Au^I](PF_6)$. *J. Am. Chem. Soc.* **2012**, *134*, 10885−10893.

(18) Luong, L. M. C.; Malwitz, M. A.; Moshayedi, V.; Olmstead, M. M.; Balch, A. L. Role of Anions and Mixtures of Anions on the Thermochromism, Vapochromism, and Polymorph Formation of Luminescent Crystals of a Single Cation, $[(C_6H_{11}NC)_2Au]^+$. *J. Am. Chem. Soc.* **2020**, *142*, 5689−5701.

(19) Luong, L. M. C.; Lowe, C. D.; Adams, A. V.; Moshayedi, V.; Olmstead, M. M.; Balch, A. L. Seeing luminescence appear as crystals crumble. Isolation and subsequent self-association of individual

[$(C_6H_{11}NC)_2Au$]$^+$ ions in crystals. *Chem. Sci.* **2020**, *11*, 11705−11713.
(20) Luong, L. M. C.; Olmstead, M. M.; Balch, A. L. A Non-Luminescent Polymorph of [(Cyclohexyl Isocyanide)$_2$Au]PF_6 that Becomes Luminescent Upon Grinding or Exposure to Dichloromethane Vapor. *Chem. Commun.* **2021**, *57*, 793−796.
(21) Lim, S. H.; Olmstead, M. M.; Balch, A. L. Molecular Accordion: Vapoluminescence and Molecular Flexibility in the Orange and Green Luminescent Crystals of the Dimer, Au_2(μ-bis(diphenylphosphino)ethane)$_2Br_2$. *J. Am. Chem. Soc.* **2011**, *133*, 10229−10238.
(22) Lim, S. H.; Olmstead, M. M.; Balch, A. L. Inorganic topochemistry. Vapor-induced solid state transformations of luminescent, three-coordinate gold(I) complexes. *Chem. Sci.* **2013**, *4*, 311−318.
(23) Al-Baker, S.; Hill, W. E.; McAuliffe, C. A. Novel Ring Compounds of Bidentate Phosphines with Gold(I). Two-, Three-, and Four-co-ordination. *J. Chem. Soc., Dalton Trans.* **1985**, 2655−2659.
(24) Yau, J.; Mingos, D. M. P. Synthesis and applications of [$Au(NCPh)_2$]$^+$, a versatile labile gold(I). *J. Chem. Soc., Dalton Trans.* **1997**, 1103−1111.
(25) Schuh, W.; Kopacka, H.; Wurst, K.; Peringer, P. Observation of a P/M interconversion of a gold−phosphine helicate via ^{31}P NMR. *Chem. Commun.* **2001**, 2186−2187.
(26) Kim, J. H.; Reeder, E.; Parkin, S.; Awuah, S. G. Gold(I/III)-phosphine complexes as potent Antiproliferative Agents. *Sci. Rep.* **2019**, *9*, No. 12335.
(27) Ecken, H.; Olmstead, M. M.; Noll, B. C.; Attar, S.; Schlyer, B.; Balch, A. L. Effects of anions on the solid state structures of linear gold(I) complexes of the type (*o*-xylyl isocyanide)gold(I) (monoanion). *J. Chem. Soc., Dalton Trans.* **1998**, 3715−3720.
(28) White-Morris, R. L.; Olmstead, M. M.; Jiang, F.; Tinti, D. S.; Balch, A. L. Remarkable Variations in the Luminescence of Frozen Solutions of [Au{$C(NHMe)_2$}$_2$]-(PF_6)·0.5(Acetone). Structural and Spectroscopic Studies of the Effects of Anions and Solvents on Gold(I) Carbene Complexes. *J. Am. Chem. Soc.* **2002**, *124*, 2327−2336.
(29) Rios, D.; Pham, D. M.; Fettinger, J. C.; Olmstead, M. M.; Balch, A. L. Blue or Green Glowing Crystals of the Cation [Au{C(NHMe)$_2$}$_2$]$^+$. Structural Effects of Anions, Hydrogen Bonding, and Solvate Molecules on the Luminescence of a Two-Coordinate Gold (I) Carbene Complex. *Inorg. Chem.* **2008**, *47*, 3442−3451.
(30) Saitoh, M.; Balch, A. L.; Yuasa, J.; Kawai, T. Effects of Counter Anions on Intense Photoluminescence of 1-D Chain Gold (I) Complexes. *Inorg. Chem.* **2010**, *49*, 7129−7134.
(31) Streitberger, M.; Schmied, A.; Hey-Hawkins, E. Selective Formation of Gold(I) Bis-Phospholane Macrocycles, Polymeric Chains, and Nanotubes. *Inorg. Chem.* **2014**, *53*, 6794−6804.
(32) Lim, S. H.; Schmitt, J. C.; Shearer, J.; Jia, J.; Olmstead, M. M.; Fettinger, J. C.; Balch, A. L. Crystallographic and Computational Studies of Luminescent, Binuclear Gold(I) Complexes, Au_2^I(Ph_2P-$(CH_2)_n$$PPh_2$)$_2I_2$ (n = 3−6). *Inorg. Chem.* **2013**, *52*, 823−831.
(33) Bates, P. A.; Waters, J. M. The Crystal and Molecular Structure of Dichloro-1,2-bis(diphenylphosphino)-ethanedigold(I). *Inorg. Chim. Acta* **1985**, *98*, 125−129.
(34) Walters, D. T.; England, K. R.; Ghiassi, K. B.; Semma, F. Z.; Olmstead, M. M.; Balch, A. L. Steric effects and aurophilic interactions in crystals of Au_2(μ-1,2-bis(diphenylphosphino)ethane)-X_2 and Au_2(μ-1,2-bis(dicyclohexylphosphino)ethane)X_2 (X = Cl, Br, I). *Polyhedron* **2016**, *117*, 535−541.
(35) England, K. R.; Lim, S. H.; Luong, L. M. C.; Olmstead, M. M.; Balch, A. L. Vapoluminescent Behavior and the Single-Crystal-to Single-Crystal Transformations of Chloroform Solvates of [Au_2(μ-1,2-bis(diphenylarsino)ethane)$_2$](AsF_6)$_2$. *Chem.—Eur. J.* **2019**, *25*, 874−878.
(36) Balch, A. L.; Tulyathan, B. Interactions between Rhodium(I) Centers in Dimeric Complexes. *Inorg. Chem.* **1977**, *16*, 2840−2845.
(37) Krause, L.; Herbst-Irmer, R.; Sheldrick, G. M.; Stalke, D. Comparison of silver and molybdenum microfocus X-ray sources for single-crystal structure determination. *J. Appl. Crystallogr.* **2015**, *48*, 3−10.
(38) Sheldrick, G. M. SHELXT - Integrated space-group and crystal-structure determination. *Acta Crystallogr., Sect. A* **2015**, *71*, 3−8.
(39) Sheldrick, G. M. *SHELXL*, Crystal structure refinement with SHELXL. *Acta Crystallogr., Sect. C* **2015**, *71*, 3−8.

https://doi.org/10.1021/acs.inorgchem.3c01961
Inorg. Chem. 2023, 62, 15902−15911